Science of the Total Environment 468–469 (2013) S102–S116

Contents lists available at ScienceDirect

Science of the Total Environment

journal homepage: www.elsevier.com/locate/scitotenv

Modeling hydrology, groundwater recharge and non-point nitrate loadings in the Himalayan Upper Yamuna basin

Kapil K. Narula [a,*], A.K. Gosain [b]

[a] Columbia Water Center (India Office), Columbia University, New Delhi 110 016, India
[b] Department of Civil Engineering, Indian Institute of Technology (IIT) Delhi, Hauz Khas, New Delhi 110 016, India

HIGHLIGHTS

- ► Applies a framework for an integrated hydrological, hydrochemical, and groundwater quality model using SWAT–MODFLOW–MT3DMS
- ► Applies the integrated framework to a Himalayan watershed
- ► Provides calibration and validation of each of the modules, including sensitivity analysis using LH-OAT
- ► Estimates impact of climate change under various scenarios (A2, B2 and A1B for end of the century scenarios).

ARTICLE INFO

Article history:
Received 16 March 2012
Received in revised form 3 January 2013
Accepted 7 January 2013
Available online 26 February 2013

Keywords:
Climate change
Hydrology
Nitrate
SWAT
MODFLOW
MT3DMS

ABSTRACT

The mountainous Himalayan watersheds are important hydrologic systems responsible for much of the water supply in the Indian sub-continent. These watersheds are increasingly facing anthropogenic and climate-related pressures that impact spatial and temporal distribution of water availability. This study evaluates temporal and spatial distribution of water availability including groundwater recharge and quality (non-point nitrate loadings) for a Himalayan watershed, namely, the Upper Yamuna watershed (part of the Ganga River basin). The watershed has an area of 11 600 km^2 with elevation ranging from 6300 to 600 m above mean sea level. Soil and Water Assessment Tool (SWAT), a physically-based, time-continuous model, has been used to simulate the land phase of the hydrological cycle, to obtain streamflows, groundwater recharge, and nitrate (NO_3) load distributions in various components of runoff. The hydrological SWAT model is integrated with the MODular finite difference groundwater FLOW model (MODFLOW), and Modular 3-Dimensional Multi-Species Transport model (MT3DMS), to obtain groundwater flow and NO_3 transport. Validation of various modules of this integrated model has been done for sub-basins of the Upper Yamuna watershed. Results on surface runoff and groundwater levels obtained as outputs from simulation show a good comparison with the observed streamflows and groundwater levels (Nash–Sutcliffe and R^2 correlations greater than +0.7). Nitrate loading obtained after nitrification, denitrification, and NO_3 removal from unsaturated and shallow aquifer zones is combined with groundwater recharge. Results for nitrate modeling in groundwater aquifers are compared with observed NO_3 concentration and are found to be in good agreement. The study further evaluates the sensitivity of water availability to climate change. Simulations have been made with the weather inputs of climate change scenarios of A2, B2, and A1B for end of the century. Water yield estimates under climate change scenarios have been made and implications on groundwater and groundwater quality have been assessed. The delicate groundwater resource balance that connects livelihoods of millions of people seems to be under tremendously increasing pressure due to the dynamic conditions of the natural environment of the region and the future climate changes.

1. Introduction

Water is a prime natural resource, a basic human need, and a precious asset, in the absence of which, no socio-economic developmental activity can be sustained (GoI, 2012). India receives most of its annual precipitation from monsoons that occur within 3–4 months in a year. Due to high coefficient of variation in rainfall and uneven availability of good quality water, several parts of the country face water stress and scarcity (Chitale, 1992; Engelman and LeRoy, 1993; Narula and Lall, 2010).

Agriculture is the major user of water and accounts for more than 85% of the total water use for irrigation (NCIWRDP, 1999; Amarasinghe

* Corresponding author at: 101, K 62, Hauz Khas Enclave, New Delhi 110 016, India. Tel.: +91 11 2656 8528.
E-mail address: kkn2104@columbia.edu (K.K. Narula).

0048-9697/$ – see front matter
http://dx.doi.org/10.1016/j.scitotenv.2013.01.022

et al., 2008; Narula and Lall, 2010). Within irrigation, the share of groundwater in the net irrigated area is about 50–55%, and is responsible for two-thirds of the total agricultural production (INAE, 2012). Agriculture also accounts for non-point-source pollution that arises from excessive use of fertilizers.

Among various fertilizers, namely, nitrogenous, phosphatic, and potassium-based, the use of nitrogenous fertilizers in the last 50 years accounted for 60–80% of the total use (Narula and Lall, 2010). The high level of subsidy on nitrogenous fertilizers vis-à-vis phosphatic and potassium-based fertilizers has caused the nitrogen–phosphate–potassium (NPK) ratio to tilt much in favor of N and the NPK ratio stands at a distorted 7.9:2.9:1 as against an optimal of 4:2:1 (Narula et al., 2002). Out of the various nitrogenous fertilizers used, the share of urea is almost 80%. Urea's hydrolyzing property is high and hence is not retained by the soil. It gets leached to groundwater due to rainfall and irrigation water inputs and is thus distributed by the land phase of the hydrological cycle (Narula et al., 2002; Narula and Lall, 2010).

Understanding temporal and spatial distribution of water availability, governed by the land phase of the hydrological cycle, including groundwater recharge and contaminant loadings becomes imperative for the proper management and protection of valuable water resources. The land phase of the hydrological cycle distributes precipitation as well as non-point contaminants such as nitrates into components of the runoff such as surface runoff, interflow, and groundwater recharge. The impacts of fertilizer overuse in agricultural lands or withdrawing groundwater from an aquifer, etc., cannot be properly assessed unless accurate estimation of various components is successfully carried out. Subsequently, the long-term behavior of a combined hydrologic-groundwater system under various management schemes cannot be reliably estimated.

To overcome the limitations discussed above, integrated model frameworks that dynamically link various components of the land phase of the hydrological cycle with groundwater and hydrochemistry (quality) have been applied by Conan et al. (2003) and Galbiati et al. (2006). For example, a combined model based on Soil and Water Assessment Tool (SWAT) and MODular finite difference groundwater FLOW model (MODFLOW) was originally developed to address how the water management issues concerning groundwater pumping for irrigation affect stream flows in two basins in Kansas (Sophocleous et al., 1999). This approach was expanded to simulate nitrate (NO_3) concentration in surface water and the fate of leached NO_3 in groundwater with the use of a reaction/transport model (Conan et al., 2003). Both uniform recharge amount and NO_3 loadings were input to the models. Menking et al. (2003) studied the combined SWAT runoff results with previous estimates of groundwater flow. Galbiati et al. (2006) presented the application of the watershed scale model SWAT, linked with MODFLOW, to the Bonello coastal basin in northern Italy.

The methodology followed in this study further tests and applies a similar integrated approach for a Himalayan catchment in India. This is based on modeling of the general hydrology of the region and the fate of N in the unsaturated zone using SWAT (Arnold et al., 1998), groundwater flow using MODFLOW (Harbaugh and McDonald, 1996), and the fate of leached NO_3 from the unsaturated zone into the aquifer system using the Modular 3-dimensional multi-species transport model (MT3DMS) (Zheng and Wang, 1999).

Variability in various components of the land phase of the hydrological cycle as also the climate has always been a source of water stress in India. The general impacts of climate change on water resources have been brought out by the Third Assessment Report (AR3) of the Intergovernmental Panel on Climate Change (IPCC) (Gosain et al., 2006). It indicates intensification of the global hydrological cycle affecting both ground and surface water supply. IPCC's Fourth Assessment Report (AR4) has projected a 0.5–1.2 °C rise in temperature by 2020, 0.88–3.16 °C by 2050, and 1.56–5.44 °C by 2080 depending on the scenario of future development in the Indian region (South Asia) (IPCC, 2007a). Overall, the increase in temperature is likely to be higher in winter season than in the monsoon season. Precipitation is also likely to increase in all time slices in all months except during December to February (Aggarwal, 2008). There is related discussion on the magnitude of recent climate change in the Himalayan region where storage and release of water in the seasonal snow cover need to be carefully understood (Singh and Bengtsson, 2004; Immerzeel et al., 2010; Moors et al., 2011).

Changes in the total amount of precipitation, its frequency and intensity have also been predicted. However, while projections of precipitation from various regional climate models (RCMs) suggest an increase in annual mean precipitation in northern India, they lack significant trend. Several studies suggest that an ensemble of regional models needs to be implemented to assess the uncertainty in projections (Buytaert et al., 2010; Krishna Kumar et al., 2011). Moors et al. (2011) used an ensemble of 4 RCMs and IPCC AR4 multi-model Global Climate Model (GCM) ensemble to assess future uncertainty in climate for the Ganges basin. Averaged across the Ganges region, the climate simulations show consistent warming in the range of 1.0–4.0 °C between 2000 and 2050. The RCMs also suggested an increase in annual mean precipitation. However, no consistent trend could be obtained. Based on a recent detailed assessment carried out by the Indian Institute of Tropical Meteorology (IITM), Krishna Kumar et al. (2011) examined the impact of global warming on the Indian monsoon climate using Hadley Center's high-resolution regional climate model, PRECIS. Simulations quantifying uncertainty in model predictions (QUMP) were carried out for the period 1961–2098 and utilized to generate an ensemble of future climate change scenarios for the Indian region with a grid resolution of 50 km × 50 km. Three QUMP simulations viz. Q0, Q1, and Q14 from the 17-member perturbed physics ensemble were used to simulate the gross features of the Indian monsoons. Q0 refers to the unperturbed model that uses the base parameter set from which the perturbed physics parameter sets were created, and the members of the QUMP ensemble are named, Q1–Q16, according to their global climate sensitivity (Q1 being the lowest sensitivity, Q16 the highest). The model evaluation was done using daily gridded rainfall data prepared by the Indian Meteorological Department (IMD) based on observed rainfall data from 1803 stations distributed over India (Rajeevan et al., 2006). IITM study showed good skill in representing seasonal means as well as small-scale features of monsoon over India. Results from all the simulations over India, indicate a rise in mean annual surface air temperature (~4 °C), an increase in monsoon precipitation (~15%), and also in the intensity of rainfall towards 2080, relative to the baseline period corresponding to 1970s.

The climate change impact assessment on water resources can be best handled through simulation of the hydrological conditions that prevail under various projected weather conditions in an area using an integrated watershed management approach (Gosain et al., 2006). Such an approach has been applied in this study given the fact that the hydrological response is a highly complex process governed by a large number of variables such as terrain, land use, soil characteristics, and the state of moisture in the soil. Evaluation of these elements warrants a continuous time simulation so as to keep track of the changing conditions.

Given the above context, the objectives of this study are to test and validate an integrated hydrological–groundwater–hydrochemical (quality) framework for prediction of water quantity and quality in a Himalayan watershed, namely, the Upper Yamuna watershed (part of the larger Ganga river basin). The study tries to evaluate the impact of climate change on water resources and groundwater under various climate change scenarios. It attempts to improve the understanding of physical parameters that are important determinants of components of integrated hydrological–groundwater–hydrochemical modeling framework for a Himalayan watershed.

2. Material and methods

2.1. Description of the study area

The Upper Yamuna watershed lies in the north of India. The river stream, namely Yamuna, originates from the Jamnotri springs (30° 58′ N, 78° 27′ E) in the lesser Himalayan zone at an elevation of about 6320 m above mean sea level (msl). After flowing in the south-westerly direction for about 120 km, it is joined by its principal tributary, the Tons (rising from 31° 13′ N, 78° 26′ E at an elevation of 3900 m above msl). From the west, another tributary, the Giri, that rises further northwest of the Tons, joins the main river. The combined stream then forces its way through the lower Siwalik Himalayan range and enters the plains near Tajewala where a weir exists at an elevation of 600 m above msl. The total length of the river till Tajewala is 172 km. The Upper Yamuna watershed till Tajewala covers a total area of approximately 11 600 km^2 (Fig. 1).

Rainfall spells in the watershed are generally associated with monsoon or late monsoon depressions either from the Bay of Bengal or the Arabian Sea. Normally, monsoon sets in by about the end of third week of June and withdraws by about the middle or third week of September. The watershed receives about 140 cm of rainfall throughout the year, of which about 75% occurs during the three monsoon months (July–September). The probability of wet day following a wet day ranges from <0.1 in the months of November and May to >0.7 in the months of July, August, and September. Daily observed temperature shows that the minimum and maximum temperature ranges from −6 °C to 43 °C (Chander et al., 1984; IMD, 1999).

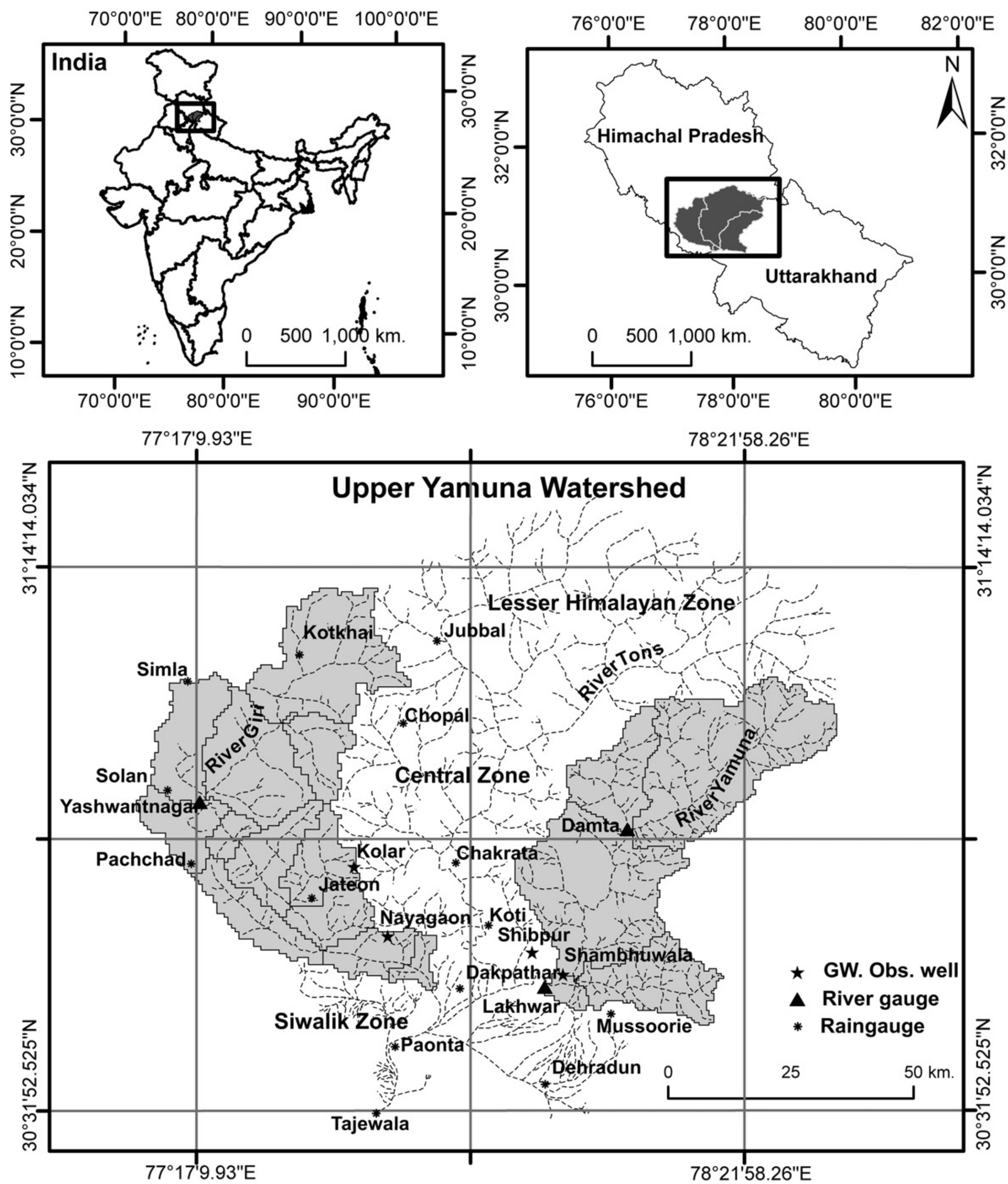

Fig. 1. Extent and location of Upper Yamuna watershed.

Hydrogeology of the watershed is divisible into the Lesser Himalayan Zone in the north, the Central Zone, and Siwalik Zone in the south (Bartarya, 1995). The Lesser Himalayan Zone consists of consolidated formations, such as quartzite, schist, phyllite, hard sandstone, limestone, and dolomite having secondary porosity. Relatively gently sloping grounds are mainly characterized by deep weathering. The groundwater in this zone occurs largely as disconnected local bodies under both confined and unconfined conditions. The sand–gravel deposits in the Lesser Himalayan Zone in the lower reaches of the stream or near confluence of two streams are highly porous and permeable and therefore, hold sufficient quantities of water. The Central Zone is occupied by the Doon gravels having primary porosity and permeability. The groundwater is present under unconfined and confined conditions. The coarse sand and gravel underlain by clay beds are the main water bearing strata. The depth of water table varies from 3 m to 100 m below ground level and hence lower or deep groundwater aquifer conditions exist in this area.

The Siwalik Zone consists of an aquifer present under lower or deep conditions and the water table is relatively deep. It consists of brown, gray, and purple gray, fine-to-coarse-grained sandstones, inter-bedded with brown and gray mudstones. The regional groundwater flow in the lower groundwater aquifers and through the colluvial deposits in the Lesser Himalayan region is south, southeast, and southwest direction. In the Siwalik Zone, groundwater flows in the north and north eastern direction (Kumar and Ghosh, 1991).

The watershed consists of six land use classes namely, forests (49%), arable land (28%), habitations (1%), rocks and wasteland (9%), grassland (11%), and orchards (2%). Crops grown in arable land include potato, wheat, maize, rice, and sugarcane. The total irrigated area is 20–22% of the arable area. The soils are mostly shallow-to-deep loamy soils with varying texture. About 50% of the watershed is characterized by moderately deep-to-deep soils where the average soil depth is more than 1000 mm (Narula, 2005). The use of fertilizers in the irrigated portions of the watershed has shown an increase from 12 000 tonnes to 30 000 tonnes between 1975 and 2005 (FAI, various issues). Fertilizer application per unit cultivable area has also increased from an average of 25 kg ha^{-1} to >85 kg ha^{-1} during the same period. The fertilizer use in the fertile area south of the watershed is 150–175 kg ha^{-1}.

The Central Pollution Control Board (CPCB) monitors water quality in the river through a network of three monitoring stations in the watershed. The NO_3 values show an increase from less than 0.6 mg l^{-1} in 1976 to 6 mg l^{-1} in 2005. Nitrate pollution is of a greater concern in case of lower groundwater. Nitrate concentrations in the agricultural areas of the watershed have increased from less than 1 mg l^{-1} in middle 1970s to 2.5 mg l^{-1} in late 1970s, 5.6 mg l^{-1} in late 1980s and more than 10 mg l^{-1} in mid 2000 (CPCB, various issues). The watershed is covered by three river-gauging stations (Yashwantnagar on river Giri, and Damta and Lakhwar on river Yamuna) for which daily-observed runoff values were available for years 1976 to 1979 for five months in a year covering the monsoon period (middle of June to middle of October). A very limited data on runoff could be obtained from the Central Water Commission (CWC) (Ministry of Water Resources, Government of India) by the Department of Civil Engineering, Indian Institute of Technology (IIT) Delhi, India, due to reasons of data confidentiality with regard to Ganga basin. All the stations are discharge-gauge stations. Similarly, the watershed is covered by four groundwater monitoring stations that measure both groundwater levels and NO_3 concentrations. Fig. 1 shows the sub-basins, location of discharge-gauge stations, and groundwater monitoring stations (observation wells).

2.2. Model principles

The integrated SWAT–MODFLOW–MT3DMS linkage uses SWAT Model (Neitsch et al., 2005) for estimating various components of the land phase of the hydrological cycle and nitrogen fate in the unsaturated zone; MODFLOW (Harbaugh and McDonald, 1996) for groundwater flow; and MT3DMS (Zheng and Wang, 1999) for assessing the fate and transport of NO_3 leached from the topsoil.

2.2.1. SWAT model

SWAT is a physically based, computationally efficient, continuous time model with spatially explicit parameterization (Arnold et al., 1996). The model sub-divides watershed into multiple sub-basins connected by stream network. It further discretizes a sub-basin according to Hydrologic Response Units (HRUs) consisting of unique soil, slope, and land use combinations. The local HRU water balance is presented by four storage volumes: snow, soil profile (0–2 m), shallow aquifer (2–20 m), and deep aquifer (>20 m). Soil profile can be subdivided into multiple layers. Soil water processes include infiltration, evaporation, plant uptake, lateral flow, and percolation to lower layers. The model offers three options for estimating potential evapotranspiration (ET), including Hargreaves, Priestley–Taylor, and Penman–Monteith methods. It computes evaporation from soil and plants separately. Percolation from the bottom of the soil profile and root zone recharges the shallow unconfined aquifer. Surface runoff from daily rainfall is estimated with a modification of the Soil Conservation Service (SCS) curve number (CN) method and Green-Ampt infiltration method. Lateral sub-surface flow in the soil profile is calculated simultaneously with percolation using kinematic storage routing technique.

Nutrient movement or transport is influenced by the land phase of the hydrological cycle. These nutrients get transported with surface runoff, lateral flow, or percolation. Nutrient uptake by plants is influenced by the fraction of potential heat units accumulated for the plant on a given day in the growing season. Nutrient transformation processes such as those for nitrogen include mineralization, nitrification and hydrolysis, volatilization, and denitrification. The kinetics of these processes is mainly influenced by soil moisture, temperature conditions as well as soil- and crop-related organic carbon (org C) and nitrogen pools. Detailed documentation on hydrological and nitrogen cycle simulated by SWAT can be found in Arnold et al. (1998) and Neitsch et al. (2005).

2.2.2. MODFLOW model

MODFLOW is a fully distributed model that calculates groundwater flow from aquifer characteristics. It solves the three-dimensional groundwater flow equation using finite-difference approximations. The finite-difference procedure requires that the aquifer be divided into cells, where the aquifer properties are assumed to be uniform. Hydraulic head (calculated as groundwater elevation derived from depth to water) in each cell is calculated at a point or node at the center of the cell. MODFLOW is designed to simulate such aquifer systems in which saturated-flow conditions exist, Darcy's Law applies, the density of groundwater is constant, and the principal directions of horizontal hydraulic conductivity or transmissivity do not vary within the system (Conan et al., 2003). More details about the model can be found in McDonald and Harbaugh (1988).

2.2.3. MT3DMS model

MT3DMS is a three-dimensional groundwater contaminant and solute-transport model used to simulate changes in concentrations of miscible contaminants in groundwater considering advection, dispersion, diffusion, and chemical reactions, with various types of boundary conditions and external sources or sinks (Zheng and Wang, 1999). The model program uses a modular structure that is represented by the cell-by-cell flow data as computed by MODFLOW to establish the groundwater flow field. The basic chemical reactions included in the model are equilibrium-controlled or rate-limited linear or non-linear sorption, and first-order irreversible or reversible kinetic reactions. Model output gives the predicted concentrations at a user-specified set of positions for specified output times. The advective–dispersive-decay solute transport equation (ADDE) is the starting step for the grid-wise formulation of this module (Zheng and Bennett, 1995) represented by Eq. (1).

$$\frac{\partial(nC)}{\partial t} = -\frac{\partial}{\partial l}(nvC) + \frac{\partial}{\partial l}\left(n\mathrm{E}_l(v)\frac{\partial C}{\partial l}\right) - K_{dn,aq}C \quad (1)$$

where, $E_{\updownarrow}(v) = \alpha_{\updownarrow} v + D_d$, and C is the contaminant concentration (g m^{-3}), n is porosity of subsurface system, D_d is the coefficient of diffusion (m^2 day^{-1}), $E_{\updownarrow}(v)$ is the coefficient of hydrodynamic dispersion (m^2 day^{-1}) in the dominant flow direction, $\alpha_{\updownarrow}$ is dispersivity (m) in the dominant flow direction, ℓ denotes the distance in the dominant flow direction (m), $K_{dn,aq}$ is the denitrification rate constant in the aquifer (day^{-1}), t is time (day), and v is the uniform or linear velocity in each grid cell (m day^{-1}). More details about the model can be found in Zheng and Wang (1999).

2.3. Input data and integrated SWAT–MODFLOW–MT3DMS model setup

Major inputs to the integrated model can be categorized into spatial and non-spatial data. Spatial datasets pertain to topography, land use, aquifer, and soil type. Non-spatial inputs include data on weather, soil properties, land use/cover characteristics, groundwater levels, fertilizer use and crops.

The following datasets were prepared (Table 1): (1) a Digital Elevation Model (DEM) with a spatial resolution of 30 m (derived from Survey of India toposheets), (2) land-use map from Landsat (ETM+) image, (3) soil map at a scale of 1:250 000 in which the physical soil layer properties (including texture, bulk density, available water capacity, saturated conductivity, soil albedo, and org C) were collected mainly from the National Bureau of Soil Survey and Land Use Planning Handbook and field data (NBSS&LUP, 1994), (4) hydrogeological and groundwater information on groundwater-bearing lithologic units, groundwater levels, fluctuations, hydrochemical data collected from the Geological Survey of India (GSI); the National Atlas and Thematic Mapping Organization (NATMO, District Planning Map Series (1996)), and the State Groundwater Board on a scale of 1: 250 000, (5) crop and fertilizer use data from the Fertilizer Statistics, Fertilizer Association of India (FAI), (6) surface and groundwater quality data from central and state pollution control boards, and (7) climate data provided from IMD climatological tables (mean monthly rainfall, maximum and minimum mean monthly air temperature, mean monthly wind speed, solar radiation, and relative humidity) and rain gauges in the watershed (daily precipitation from 14 rain gauges provided by the IMD as shown in Fig. 1; IMD, 1999).

The ArcView Interface for SWAT 2000 (Neitsch et al., 2002), was used to delineate the boundaries of the entire watershed and its sub-basins, along with their drainage channel. The boundary of the watershed was superimposed on Google Earth to ensure that delineated watershed boundary and drainage channels closely matched the mountain and hill ridges and drainage network on Google Earth imagery. Further, land use and soil map were used to define multiple HRUs for each sub-basin.

The land cover/use map was processed as raster data and included six categories as discussed in Section 2.1 from Landsat (ETM+) image. These remotely sensed data accounted for the spatial variability in forest and other vegetation characteristics. The vegetation map was finalized after field verification in each of the delineated sub-basin. The barren landcover category, which includes bare ground and rock outcrops, was parameterized by modifying the dirt road transportation parameter set in SWAT (Ahl et al., 2008). The soil databases consisting of soil map and attribute information developed by NBSS&LUP were used to characterize soils in the study area. Finally, the values for the standard soil and land use parameters used to configure the model were extracted and/or estimated from datasets by the SWAT interface.

In SWAT, these parameters are grouped at the levels of watershed, sub-basin, and HRU, and are described in detail by Neitsch et al. (2002). The number and diversity of HRUs can influence model output (Ahl et al., 2008), and to ensure a high level of resolution, multiple HRUs were defined for the watershed. Crop management parameters in SWAT were based on normal practice of farmers in the watershed. Application of nitrogenous fertilizers was incorporated using data available from Fertilizer Statistics (FAI, various issues) for the region and farmer interactions. Fertilizer used in the watershed is urea and the input varied from 80 to 175 kg ha^{-1} depending on the crop grown such as wheat, potato, generic agricultural (crop mix), and fruits. These were estimated using fertilizer statistics data available from FAI (FAI, various issues, 1970–2004) and primary data collected from field visits. Field visits revealed that wheat-growing areas applied 80–120 kg ha^{-1} urea, potato-growing areas applied 150–175 kg ha^{-1}, rice and maize 75–110 kg ha^{-1}, and fruits in general required 100–150 kg ha^{-1} urea. The fertilizer was applied twice or thrice in a season corresponding to basal, tillering and floral formations in a crop and thereby its critical growth stages. This was incorporated in SWAT

Table 1
Various datasets used and their sources.

Theme	Data basis	Source and map scale
Topography	Digital Elevation Map (DEM), stream networks	Survey of India (SoI); 1:50000
Climatic data	Mean monthly and daily precipitation, maximum and minimum temperature, solar radiation, wind speed, potential evaporation	Climatological tables (1951–1980); Daily rainfall data available for rain gauges in the watershed, Indian Meteorological Department (IMD)
Soil-physical data	Soil characteristics (% silt, sand, clay, rocks), field capacity, wilting point, hydraulic conductivity, depth to water table, properties for different soil layers varying with depth	National Bureau of Soil Survey and Land use planning (NBSS&LUP); 1:250 000; National Thematic Map Organization (NATMO)
Land use data	Ground cover	SoI, Landsat (ETM+) image, State Agricultural Board, 1:50 000 and 1:250 000
Hydrogeological data and groundwater fluctuation	Groundwater-bearing lithologic units, transmissivity, hydraulic conductivity, groundwater levels, fluctuations, hydrochemical data, water use (pumping and extraction)	Geological Survey of India (GSI); NATMO, central and state groundwater boards, 1:250 000
Gauge data	Daily river flows	Chander et al. (1984), Central Water Commission, Ministry of Water Resources
Crop and fertilizer data	Nitrogenous fertilizers use, crop yields and types of crops; gross and net cropped areas	Fertilizer Statistics, Fertilizer Association of India (FAI)
Water quality data	Surface water quality (nitrate concentrations), ground water quality (nitrate concentrations)	Central Pollution Control Board (CPCB); State Pollution Control Board (SPCB), Station-wise data

based on accumulated heat units (the fraction of total base zero heat units at which the stage/operation takes place) of 0.05, 0.25, and 0.5 (Williams et al., 1984).

Precipitation in mountainous watersheds is influenced by changes in elevation. Fontaine et al. (2002) showed that definition of elevation bands within the model's sub-basins can enhance simulation performance in watersheds with topography having large elevation gradients. Elevation bands were defined to account for a high elevation gain. The data collected from 14 rain-gauge stations has a record of daily precipitation from 1969 to 1988. Data from these rain gauges and from the National Weather Station maintained by IMD were used to estimate the local precipitation lapse rate. Once established, these values were used to parameterize SWAT and then maintained throughout the calibration.

The data on daily precipitation were pre-processed into database files within the SWAT required format. Long term (1951–80) mean monthly values on rainfall, solar radiation, wind speed, relative humidity, and number of precipitation days in a month obtained from IMD (1999) for stations Simla, Mussoorie, and Dehradun, were used as inputs into the weather generator (a stochastic engine incorporated in the deterministic SWAT software package). The missing values on daily precipitation were simulated by the calibrated and validated weather generator using the procedures described by Neitsch et al. (2002).

Further, during the simulation period, records on daily streamflows were available for various stations (Fig. 1) in the watershed for a period of four years (1976–79) for five months in a year (June–October) covering the complete monsoon cycle. Three year data that is, 1976–78 was used for calibration and data for 1979 was used for validation purposes. Similarly, records on surface water quality with regard to NO_3 concentrations observed over the same time period were used for calibration and validation of NO_3 loadings in the watershed.

After successful validation of the land phase of the hydrological cycle, the MODFLOW model was set-up coupled to SWAT. The hydrologic terms simulated by SWAT for each sub-basin were transformed to the system of units specified for MODFLOW's simulation. Grid cells of MODFLOW were associated with geographical extent of sub-basins simulated by SWAT. Groundwater limits for the model correspond to those of the surface water basin. These boundaries were designated as no flow boundaries. The properties of aquifer material including hydraulic conductivity, storage coefficient, specific yield, and transmissivity were provided into the model. The study made use of geostatistical and stochastic technique in deriving spatial distribution of aquifer parameters. Stochastic technique has been used for estimating effective porosity of the rocks mainly to ensure that the final values assigned to the two parameters — hydraulic conductivity and effective porosity — achieve a bivariate distribution (Kunkel and Wendland, 1997). The information on aquifer thickness was extracted from lithological information (strata charts) available in terms of borehole logs (collected from state and central groundwater boards). Digital maps showing top and bottom elevations of the individual geological layers and lenses were generated from borelogs in Groundwater Modelling System (GMS) version 5.1. Spatial distribution of various aquifer parameters such as bottom and top elevations, starting heads, hydraulic conductivity, effective porosity, and transmissivity on a regional basis was finally estimated using the above methods. The hydraulic conductivity used in the model ranged from 10^{-5} to 3.10^{-4} ms^{-1}, and the specific yield used in the model ranged from 0.01 to 0.15. The specific storage ranged from 3.10^{-3} to 10^{-4}. All these calibrated values were found to be within the range of literature values given for this watershed (SGWB, 1982).

Hydrologic components simulated by SWAT for each sub-basin were combined to specify fluxes for MODFLOW's solution in each time step and distributed to each corresponding grid cell (Sophocleous et al., 1999). These fluxes mainly included groundwater recharge (Conan et al., 2003). Recharge to a model cell was specified as recharge intensity, a SWAT output, and has dimensions of velocity. The recharge flux was estimated by multiplying the intensity with the grid cell area of MODFLOW. The well package of MODFLOW that simulates pumping or injection wells uses rates specified for each time period of the simulation independent of both the cell area and the head in the cell.

The model was initially calibrated under steady state conditions by adjusting input data including hydraulic conductivity and vertical conductance. Calibration under transient conditions also included adjustment of specific yield and storage. Records on monthly groundwater levels were available for various stations in the watershed covering the same time period and used for calibration and validation of MODFLOW.

Finally, the MT3DMS model was set up based on the grid inputs and results of MODFLOW. Distributed NO_3 loads calculated by SWAT were provided as input for each time period. Since NO_3 neither precipitates nor is adsorbed and does not form insoluble materials, the only natural way of removing it from aquifers is by reduction (Chapelle, 1993; Conan et al., 2003) in MT3DMS. The concentration and availability of dissolved oxygen (O_2), organic matter, divalent manganese (Mn(II)), and/or pyrite (FeS_2) were used to determine the denitrification process. Groundwater data suggests that the aquifer is mostly a non-nitrate degrading type mainly due to the absence of divalent iron (Fe(II)) and Mn(II) that occur as a rule in reduced groundwater conditions in concentrations >0.2 and 0.05 mg l^{-1} (Wendland, 1992, 1994). In other words, these aquifers can be categorized as sensitive to NO_3 inputs. Nitrate reduction was modeled in MT3DMS by a first-order irreversible reaction (Conan et al., 2003). The first-order rate constant was estimated to be as low as 5.10^{-4}–10^{-3} d^{-1} for the weathered rocks and 0.04–0.07 d^{-1} for the schists. This coefficient, corresponding to a half-life time of 12 d, was in agreement with the half-life time of 11 d calculated by Conan et al. (2003) and 8 d by Pauwels et al. (1998). All calibrated physical and hydrogeological parameters of the models were kept the same as presented in the previous sections. Records for groundwater quality were available for various stations in the watershed and were used for calibration and validation of MT3DMS.

2.4. Model calibration and validation

The original design objective of the SWAT model was to operate in large-scale, ungauged basins with little or no calibration efforts (Arnold et al., 2000; Arnold et al., 1998). Studies have demonstrated that SWAT input parameter values can be successfully estimated with or without minimum calibration in a wide variety of hydrologic systems and geographic locations using readily available GIS databases that have been developed based on prior knowledge (Srinivasan et al., 1998; Arnold and Allen, 1999; Gosain et al., 2005; Zhang et al., 2008; Shi et al., 2011).

Calibration has been undertaken by conducting a sensitivity analysis to identify surface runoff, groundwater levels, and nutrient loading related parameters that are sensitive for simulation. Guidance for identifying input parameters for calibration and sensitivity analysis was provided by prior research in agricultural and mountainous catchments by Garg et al. (2011), Abbaspour et al. (2007), Gosain et al. (2005), Holvoet et al. (2005), Arnold et al. (1998) and Srinivasan et al. (1998).

Following manual calibration based on understanding of the watershed, sensitivity analysis was also implemented using Latin Hypercube-One-factor-At-a-Time (LH-OAT) (van Griensven et al., 2006; van Griensven, 2005). LH sampling is computationally efficient, and OAT procedures ensure that a change in model output is unambiguously attributed to the change in an input parameter (Ahl et al., 2008). LH-OAT starts with taking *N* LH sample points for *N* intervals, it then varies each LH sample point *P* times by changing each of the parameters one at a time. The method operates by loops and each loop starts with an LH point. Around each LH point j, a partial effect S_{ij}, for each parameter e_i is calculated as in Eq. (2):

$$S_{ij} = \left| \frac{100 * \left(\frac{M(e_1, \ldots e_i*(1+f_i), \ldots e_p) - M(e_1, \ldots e_i, \ldots e_p)}{[M(e_1, \ldots e_i*(1+f_i), \ldots e_p) + M(e_1, \ldots e_i, \ldots e_p)]/2} \right)}{f_i} \right| \quad (2)$$

where M(…) refers to model functions, f_i is the fraction by which the parameter e_i is changed (a predefined constant) and j refers to a LH point. A final effect is calculated by averaging the partial effects of each loop for all LH points. The final effects can be ranked with the largest effect being given rank 1 and the smallest effect given rank equal to the number of parameters. Thus, the impact of each parameter on the model results can be quantified and the most sensitive parameters can be identified (Li et al., 2009).

For this study, calibration and validation of the runoff component of the land phase of the hydrological cycle model were obtained by using daily observed surface flow data. Three year data, that is, 1976–78, was used for calibration and data for 1979 was used for validation purposes. Calibration and validation of groundwater recharge were obtained by using monthly observed groundwater elevation data for the same time period. Nitrate loads in relation to surface water quality were calibrated by using observed surface water quality data. Nitrate concentrations in groundwater aquifer were simulated based on the contaminant leaching from the land-based application of excess fertilizers into the aquifer. The obtained results were compared with the observed groundwater quality data. Thus, the calibration process for the integrated model was made for four components namely, streamflow, groundwater recharge, NO_3 loads in relation to surface water quality, and NO_3 fate and transport in groundwater.

Evaluation of model performance during the calibration and validation periods was done following the methods used by Neitsch et al. (2001) and Shi et al. (2011), which are coefficient of determination (R^2), and Nash–Sutcliffe efficiency (E_{NS}). R^2 is calculated according to Eq. (3).

$$R^2 = \left[\frac{\sum_{i=1}^{n} \left(O_i - \overline{O}\right)\left(S_i - \overline{S}\right)}{\sqrt{\sum_{i=1}^{n} \left(O_i - \overline{O}\right)^2} \sqrt{\sum_{i=1}^{n} \left(S_i - \overline{S}\right)^2}} \right]^2 \quad (3)$$

where, O_i is observed data value, $\overline{O}$ is the mean observed value, S_i is the simulated value and $\overline{S}$ is the mean simulated value. R^2 ranges between 0.0 and 1.0. Higher values mean better performance.

E_{NS} is calculated according to Eq. (4).

$$E_{NS} = 1.0 - \sum_{t=1}^{T} (O_i - S_i)^2 / \sum_{t=1}^{T} \left(O_i - \overline{O}_i\right)^2 \quad (4)$$

E_{NS} indicates how well the plot of the observed values versus simulated values fits the 1:1 line and ranges from -∞ to 1 (Nash and Sutcliffe, 1970). Larger E_{NS} values (close to 1) are equivalent to better model performance.

2.5. Climate change scenarios

The calibrated SWAT model has been used to assess climate change impacts using various scenarios namely, HadRM3–RCM with two emission scenarios of A2 and B2 and PRECIS–RCM with emission scenario of A1B. The model run under HadRM3 scenarios provides the projected changes for the End-Century (EC) period 2071–2100 with respect to the baseline period (BL) 1961-90. Similarly, the model run under PRECIS scenario provides the projected changes for the EC period 2071-98 with respect to BL period 1961-90. Q14, QUMP ensemble has been used for the PRECIS simulation.

Each scenario assumes a distinctly different direction for future developments. IPCC Special Report on Emission Scenarios (SRES) A2 describes "a very heterogeneous world with continuously increasing global population, regionally oriented economic growth that is more fragmented and slower than in the other story lines". IPCC SRES B2 describes "a world in which emphasis is on local solutions to economic, social, and environmental sustainability, with continuously increasing global population at a rate lower than A2, intermediate levels of economic development and more diverse technological change". Similarly, IPCC SRES A1B describes "a future world of very rapid economic growth, global population that peaks in mid-century and declines thereafter, and rapid introduction of new and more efficient technologies" (IPCC, 2000).

Precipitation under climate scenarios simulated by the HadRM3–RCM A2 and B2 suggest a 25–45% and 20–35% increase respectively from the baseline. Similarly, precipitation under PRECIS–RCM A1B scenario is projected to increase by 20–30% (Gosain, et al., 2011). Seasonal analysis shows that precipitation in summer monsoon months (also called South West monsoon from mid June till early September) is projected to increase more in the A2 than in the B2 scenario. On the other hand, precipitation during the winter months (November till February) is projected to decrease in A2 while it is projected to increase in the B2 scenario. According to studies by WWF (2010) and Moors et al. (2011) on the Ganga basin (comprising the Yamuna watershed) while projections of precipitation do indicate an increase in annual mean precipitation, a sufficient trend is lacking and natural variability seems to dominate the climate change signal.

A2, B2, and A1B scenarios show a warming up in the Upper Yamuna watershed. Climate change is projected to increase the temperatures more in A2 scenario than in B2 scenario compared to the baseline. Various studies such as Moors et al. (2011), and WWF (2010) have also indicated that the mean annual temperature under various scenarios is projected to increase in the range of 1.0–4.0 °C from the baseline. The projected increase in temperature is relatively higher during the winter months (November till February) than in the summer monsoon season. Mean maximum temperature for A2 scenario is projected to increase by 3.0–3.5 °C for the summer monsoon months and 5.0–5.25 °C during the winter season. Similarly, mean minimum temperature is projected to increase by 3.0–3.25 °C in the monsoon season as compared to 4.0–5.25 °C during winter season. As far as B2 scenario is concerned, mean maximum temperature during monsoon season is projected to rise in the range of 2.5–2.75 °C while the mean minimum temperature is projected to increase by 2.0–2.5 °C. During the winter season, an increase in mean maximum temperature is projected to be in the range of 2.5–2.75 °C, while the increase in the mean minimum temperature is projected to be in the range of 3.25–3.5 °C (WWF, 2010; Krishna Kumar et al., 2011).

The potential impacts of climate change on stream flows and other hydrologic budget components are quantified by performing integrated modeling with current and future climates, respectively. The study first determines the water availability in space and time under baseline conditions and compares them with observed flows. The same framework is then used to predict the impact of climate change on the water resources with the assumption that the land use shall not change over time. A total of 60 years of simulation has been conducted under each of the scenarios; 30 years each belonging to IPCC SRES A1B baseline and EC climate scenario; and IPCC SRES A2 and B2 baseline and EC A2 and B2 scenarios.

3. Results and analysis

Detailed outputs of integrated hydrological-hydrochemical-groundwater quality model have been analyzed with respect to major water balance and quality components namely, stream flow, groundwater recharge, NO_3 loads in relation to surface water quality, and NO_3 fate and transport in groundwater. This involves calibration and validation of various modules of the integrated model. For calibration, key parameters in the hydrologic module, nutrient module, as well as the groundwater quality module are determined and their sensitivity is discussed. Recent literature discusses similar approach used for calibration and validation of SWAT that combines major hydrological and nutrient transport components as check points for partially gauged and ungauged basins (Gassman et al., 2007; Srinivasan et al., 2010). It is also well documented that the SWAT model does not require elaborate calibration if the basic characteristics of the basin are incorporated properly (Gosain et al., 2011).

The analysis has also been extended to understand potential impacts of climate change on the above components by considering various scenarios namely A2, B2, and A1B (EC) with respect to the baseline scenario. All the analysis has been performed by aggregating the inputs/outputs at the sub-basin level that are the natural boundaries controlling the hydrological and hydrochemical processes (Arnold et al., 2000). Accordingly, calibration of the watershed has been done at the sub-basin level for Lakhwar and Giri sub-basins of the Upper Yamuna watershed comprising of three discharge gauge stations namely, Damta (upstream station in Lakhwar sub-basin), Lakhwar (downstream station in Lakhwar sub-basin) and Yashwantnagar (station in Giri sub-basin).

3.1. Integrated hydrologic–groundwater–quality simulation

The integrated SWAT–MODFLOW–MT3DMS model has been applied on the Upper Yamuna watershed. Figs. 2–4 show the measured and simulated daily discharges for three gauging stations in the watershed namely, Damta, Lakhwar and Yashwantnagar both for calibration and validation periods. The model performance evaluated using Nash–Sutcliffe coefficient (E_{NS}), and coefficient of determination (R^2) has been shown in Table 2.

Sensitivity analysis of various input parameters showed that combination of snowmelt and snow-formation as well as soil-land use parameters are the most sensitive parameters that affected streamflow. The parameters that were used for calibration include a lag factor that accounts for snow-pack characteristics, and the melting rate of snow (maximum and minimum melt factors). The temperature lag factor (TIMP) controls the influence of the previous day's temperature on the current day's snow-pack temperature and melt parameters represent maximum (SMFMX) and minimum (SMFMN) melting values that occur on the summer and winter solstices, respectively. This agrees with the findings of the study on hydrological sensitivity of Himalayan basin by Singh and Bengtsson (2004) that found seasonal changes in distribution of water availability as a result of melt runoff to be quite pronounced.

Among the soil–land use parameters, CN, which is related to both soil and vegetation, and surface runoff lag (SURLAG) related to time of concentration applicable to large sub-basins, were found to be important sensitive parameters in the model (Table 3). Another important parameter is Available Water Capacity (AWC) of the soil that determines surface runoff and ET in relation to soil storage (Arnold et al., 2000). Soil Evaporation Compensation factor (ESCO), which adjusts depth distribution for evaporation from the soil to account for capillary action, crusting and cracking, was also found to be sensitive. Variations in values of various other parameters did not further improve the results and showed moderate-to-low sensitivity in terms of adjusting flows in the study area. The results of the sensitivity analysis agree with Arnold et al. (2000), and van Griensven et al. (2006) that show hydrologic budget components to be sensitive to CN, AWC, and ESCO.

Simulation of groundwater required accurate estimations on groundwater recharge (an outcome of SWAT) and hydraulic heads for calculating groundwater flow direction, and hydraulic gradient. Aquifer hydraulic conductivity (K) and storativity/specific yield are primary calibration parameters for estimating groundwater flow (Sophocleous et al., 1999). Calibration procedure involved estimating the specific yield/storativity and comparison of recharge (RCHRG_DP) and outflows (Qaq) from groundwater aquifer, such that the resulting net recharge produced water levels are comparable with the observed values. Water use by month from aquifers was estimated for various sub-basins from the data provided by the state and central groundwater boards and entered in the water use data input file. The calibration of storage coefficient (SPYLD) was performed by developing a simple algorithm based on Smedema and Rycroft equation of groundwater recharge (Smedema and Rycroft, 1983; Arnold et al., 1998; Neitsch et al., 2000; Krysanova and Becker, 2000).

The simulation results on groundwater levels obtained during the calibration and validation periods for four observation wells (Shambhuwala, Shibpur, Kolar, and Nayagaon) are shown in Fig. 5. These have been compared with the observed datasets for estimating model performance shown in Table 2. The results of the sensitivity analysis of various parameters are shown in Table 4. Aquifer hydraulic conductivity (K) and transmissivity (T) that define the movement of groundwater, as well as net groundwater recharge i.e., net of groundwater recharge (RCHRG_DP) and discharge (Qaq), were identified to be important sensitive parameters.

Calibration of NO_3 loading is carried out after calibrating hydrological components since the land phase of the hydrological cycle influences the transport and transformation of NO_3 in topsoil. The distribution of NO_3 in soil makes use of SWAT-predefined functions (Neitsch et al., 2001) and an understanding of the watershed regarding chemical inputs (fertilizer application) and soil characteristics

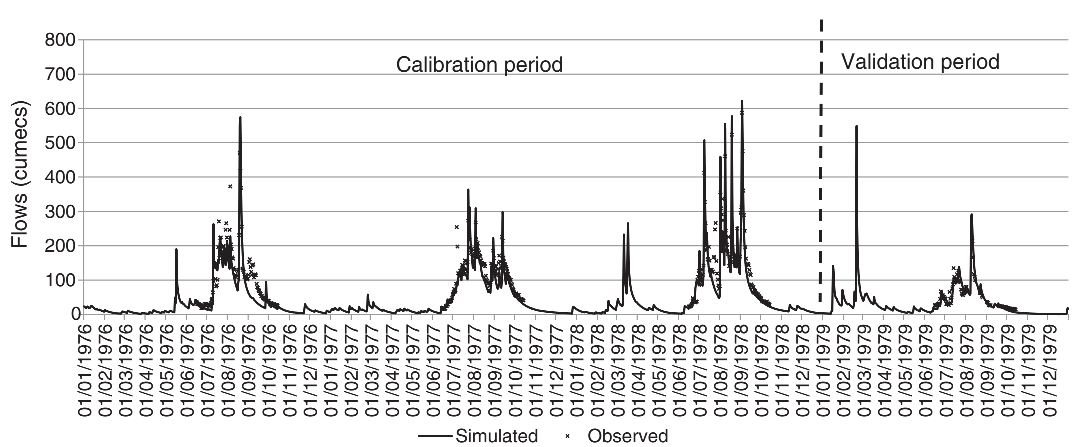

Fig. 2. Observed and simulated daily discharges (cumecs) for Damta (upstream station in Yamuna sub-basin) for calibration (1976–78) and validation (1979) periods.

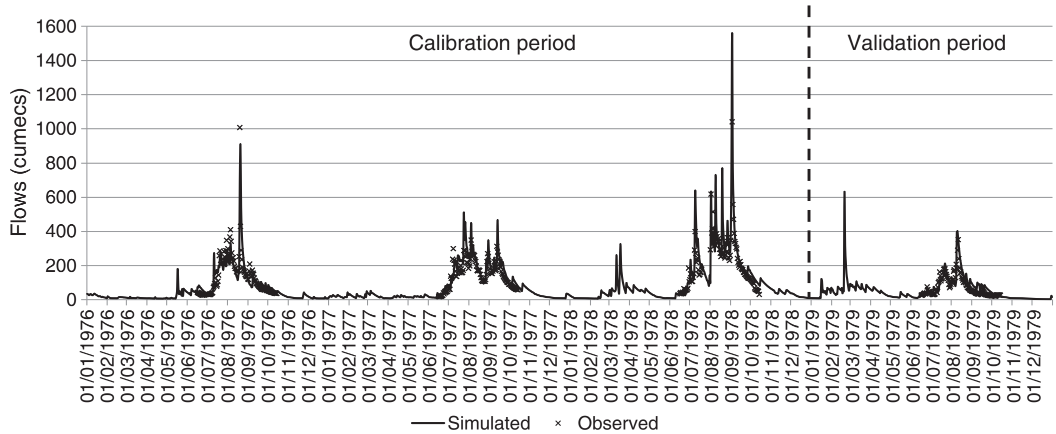

Fig. 3. Observed and simulated daily discharges (cumecs) for Lakhwar (downstream station in Yamuna sub-basin) for calibration (1976–78) and validation (1979) periods.

(initial concentrations (SOL_NO$_3$) and drainage conditions) in addition to the type of fertilizer added on soil surface (FRT_LY), depth distribution factor, and percolation factor (NPERCO) influencing transport of NO$_3$.

Simulation results and model performance of NO$_3$ in surface water are shown for two stations Lakhwar and Yashwantnagar (Figs. 6 and 7). Since there are no observed data sets for NO$_3$ loads, observed NO$_3$ concentrations available as mean daily concentrations (mg l^{-1}) for each year (CPCB, Central Pollution Control Board, 1974–2000) have been used here for comparison. The maximum, minimum and mean daily observed and simulated NO$_3$ concentrations for the calibration and validation periods are shown in Figs. 6 and 7. The sensitivity analysis of various parameters shows that NPERCO that influences the transport of nitrates, and initial concentration in soil layer (SOL_NO$_3$) is a high sensitive parameter (Table 4).

Finally, the simulated NO$_3$ concentrations obtained from MT3DMS (MODFLOW) and the observed data have been compared. Calibration of this module was carried out after successfully calibrating hydrological components (recharge) and NO$_3$ loads in the land phase of the hydrological cycle. Excess NO$_3$ leaches down from the last layer of the soil into the shallow aquifer and from the shallow aquifer to the lower aquifer. The denitrification rate coefficient (K$_v$) in aquifer was calibrated using hydrochemical characteristics of the aquifer and potential denitrification rate. In general, the aquifer is found to be a non-reducing or NO$_3$ non-degrading type suggesting a low rate of denitrification. Initial NO$_3$ concentration in the aquifer (GW_NO$_3$) was taken as those observed in the beginning of 1976. Contaminant transport properties such as longitudinal dispersivity (α_l) and coefficient of dispersion (E$_l$) were also incorporated. Final NO$_3$ concentrations simulated over a time period of 1976–79, covering calibration and validation period, were compared with the observed NO$_3$ concentration in the aquifer for 1979 and were found to be ranging between 12 and 15 N-NO$_3$ (mg l^{-1}) in the southern Siwalik agricultural belt of the watershed. Performance was determined by applying R^2, and Nash and Sutcliffe coefficient of model performance shown in Table 2. Among various parameters, denitrification rate coefficient (K$_v$) in aquifer was found to be very sensitive.

3.2. Hydrologic simulation under climate change scenarios

The integrated model has been applied using daily weather generated by the PRECIS–RCM A1B BL (1961–90), A1B EC (2071–98), SRES A2 EC (2071–2100), and SRES B2 EC (2071–2100) scenarios without changing the land use. The study first determines the water availability under baseline conditions and then compares them with observed flows. This is to confirm if the water availability outcomes from baseline correspond well with the historical observed data. The performance criteria namely R^2 and E_{NS} are found to be close to 0.6 on a monthly time step.

The same framework is then used to predict the impact of climate change on the water resources under various scenarios. The outputs from these scenarios have been analyzed with respect to likely impacts on streamflow, actual ET, NO$_3$ loads and groundwater.

Hydrological model results, on both annual and seasonal scales, show that ET increases under all the scenarios, ranging from 5% to 15% from baseline. Gosain et al. (2011) also report an increase of 10–14% in ET values compared to the baseline under A1B scenario for the Yamuna watershed.

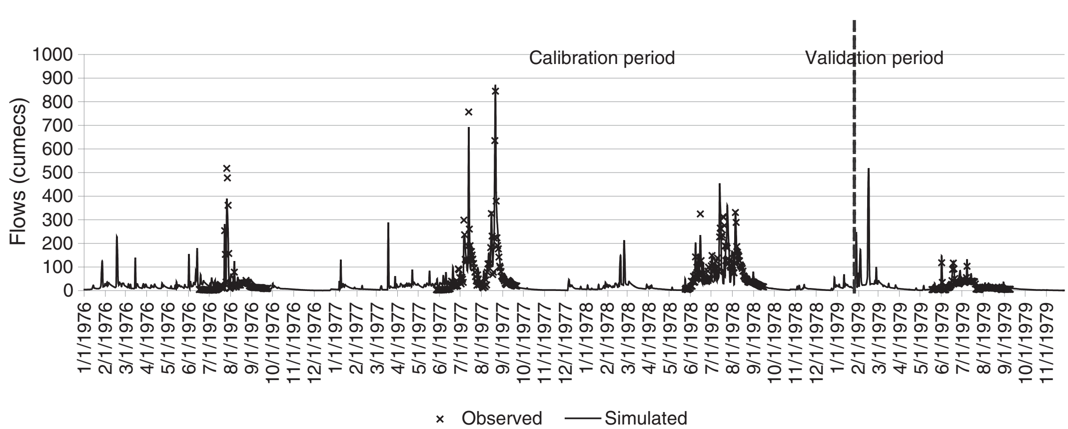

Fig. 4. Observed and simulated daily discharges (cumecs) for Yashwantnagar (Giri sub-basin) for calibration (1976–78) and validation (1979) periods.

Table 2
Model performance for streamflows and groundwater (recharge and quality) during calibration and validation periods.

Component	Calibration		Validation	
	R^2	Nash and Sutcliffe	R^2	Nash and Sutcliffe
Stream flow				
Damta upstream on River Yamuna	0.88	0.83	0.76	0.71
Lakhwar downstream on River Yamuna	0.72	0.70	0.73	0.71
Yashwantnagar on River Giri	0.79	0.76	0.79	0.75
Groundwater recharge				
Kolar	0.89	0.89	0.88	0.84
Shibpur	0.89	0.88	0.77	0.75
Shambhuwala	0.89	0.88	0.76	0.75
Nayagaon	0.88	0.89	0.88	0.84
Groundwater quality in aquifers				
Lakhwar sub-basin	0.94	0.94	0.89	0.89
Giri sub-basin	0.96	0.96	0.81	0.81

The implications of changes in precipitation and temperature have been quantified in the form of resulting water yields (or streamflows). There is an increase in average annual water yield under all the scenarios ranging from 20% to 60% for Lakhwar sub-basin, and 10–40% for Giri sub-basin compared to the baseline. Gosain et al. (2011) also report an increase in water yield by 20–35% from the baseline under A1B scenario for the Yamuna watershed. Seasonal analysis shows that water yield during monsoon season increases by 60–80% for Lakhwar and 40–60% for Giri sub-basin. Water yield decreases by 30–35% from the baseline during the winter season under A2 scenario but increases under A1B scenario while B2 scenario shows a mixed result. Under climate change scenario B2, the timing of the maximum flow period is earlier than that under baseline conditions. Whereas, under the A1B scenario it lags by certain duration compared to baseline. From an overall perspective, the above analysis implies that the seasonal variability in the availability of water is likely to increase, influenced both by natural and climate induced variability in precipitation. Several recent studies have also indicated a wide range of future seasonal streamflow changes using different climate change scenarios over northern India, and Himalayan river systems in particular, with much uncertainty in the contribution from climate change (Singh and Bengtsson, 2005; WWF, 2010; Gosain et al., 2011).

Since, nitrogen load is closely associated with streamflow, climate change also has a significant impact on it. Similar to streamflow, nitrogen loads under future climate change scenarios also increase by 40–50% over the baseline in the monsoon months but decrease by 15–30% in winter months compared to those in baseline periods. The annual nitrogen load is found to increase on an average by 15%, although the effect is relatively smaller than that on the seasonal values.

Decline in groundwater table has been observed in many parts of the watershed mainly attributed to irrigation and other anthropogenic use. The trend in lowering groundwater tables in combination with the increasing variability in precipitation and increased ET is likely to impact groundwater availability. The analysis under various scenarios shows that the percentage contribution of groundwater to total water yield would decline by 15–20% and thereby would result in lowering groundwater tables in the watershed. This is further corroborated by Kelkar et al. (2008) and Gosain et al. (2011) who report a decline in groundwater tables, an increase in the occurrence of drought weeks and soil moisture stress ranging between 10% and 20% above the baseline under A1B scenario despite the overall increase in precipitation for the Yamuna watershed. Krishna Kumar et al. (2011) have also reported that while the projected change in the number of rainy days may be non-uniform, the intensity of rainfall on a rainy day is likely to be higher in future. Rainfalls of a higher intensity would lead to increase in surface runoff and reduction in the time for percolation and recharge.

Assuming the baseline conditions for NO_3 loadings to remain the same, the likelihood of NO_3 concentrations both in the surface and groundwater of the Upper Yamuna watershed would increase further occurring as a result of either higher wash-off from high-intensity rainfall (an impulse input function) or groundwater leaching during winter crop season (a step input function). Findings of WWF (2010) study for Upper Yamuna watershed also states that the farmers will have to increase the efficiency of nitrogen and irrigation use even when they continue to grow the current crop varieties, both under A2 and B2 EC scenarios. An increased loss of N due to volatilization and other factors like additional but balanced fertilizer input is anticipated.

4. Discussion

The present study focused on quantification and analyses of various components of the land phase of the hydrological cycle including groundwater recharge and nutrient transport in the Upper Yamuna watershed by making use of integrated SWAT–MODFLOW–MT3DMS model. The integration makes it possible to analyze these components using a physically-based approach varying both spatially and temporally. The degree of accuracy of the results from integrated models needs to correspond to the local environmental situations, which requires an area-differentiated interpretation. This makes use of regional interaction of site conditions, soil, geology, and land use, as discussed below.

An area-differentiated interpretation of hydrologic budget components, namely, direct runoff (discharge) and recharge shows that the

Table 3
Results of sensitivity analysis of various parameters — surface and sub-surface modules.

Parameter	Description	Range used		Sensitivity	Rank
		Min	Max		LH-OAT
SMTMP (°C)	Threshold temperature for snowmelt to occur	−3	1	Moderate	5
SMFMX (mm °C day^{-1})	Maximum melt factor	3	3.5	Moderate	7
SMFMN (mm °C day^{-1})	Minimum melt factor	1.5	2.5	Moderate	8
TIMP	Snowpack temperature lag factor	0.03	0.065	High	1
SFTMP (°C)	Snowfall temperature threshold	0.5	1	Moderate	9
Curve number (CN2)	Curve number for moisture condition II	25	75	High	2
ESCO	Soil evaporation compensation factor	0.40	0.75	High	4
AWC (mm mm^{-1}) varying with depth	Available water capacity for soil	0.07	0.18	Moderate	6
SOL_K (mm h^{-1}) varying with depth	Soil hydraulic conductivity	20	250	Moderate/low	10
CH_K2 (mm h^{-1})	Channel conductivity	0	45	Low	11
GW_DELAY (days)	Groundwater delay time	1	65	Low	12
SURLAG	Surface lag coefficient	0.5	6	High	3

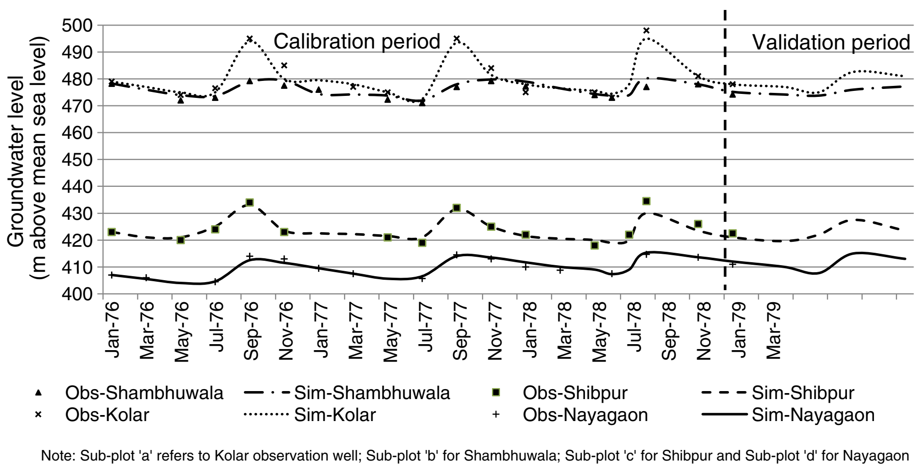

Fig. 5. Observed and simulated groundwater elevations for calibration (1976–78) and validation (1979) periods. Note: sub-plot 'a' refers to Kolar observation well; sub-plot 'b' for Shambhuwala; Sub-plot 'c' for Shibpur and sub-plot 'd' for Nayagaon.

Lesser Himalayan Zone in the northern part of the watershed (Fig. 1) forms the discharge area where direct runoff is the dominant component of the land phase of the hydrological cycle. This zone mainly consists of consolidated formations with very low intergranular porosity. The Central Zone of the watershed, characterized by high infiltration rate, forms a recharge area where groundwater recharge is the dominant component of the land phase of the hydrological cycle. This zone is mainly occupied by the Doon gravels and forms the main aquifer. The Siwalik Zone in the south forms recharge and discharge areas depending on the depth to groundwater table.

An area-differentiated interpretation further reveals that areas in the watershed that serve as good recharge areas in the central and south of the watershed are also those that are mainly characterized by moderately deep-to-deep coarse loamy soils, where average soil depth is more than 1000 mm. These soils are also characterized as well drained and moderately well drained, where water is removed from the soil matrix readily and not rapidly or at a moderately slow rate to keep the subsoil wet for a sufficient part of the growing season. These soils exhibit a wide range of available water capacity, textures, and depth. Findings from the analysis reveal that during low-flow conditions this part of the watershed exhibits higher specific discharge values compared to the northern zone due to regional groundwater discharges. Conversely, during high flow conditions the southern part of the watershed exhibits low specific discharges in comparison to northern parts of the watershed. For instance, Damta (an upstream station of the watershed) shows higher specific discharge during monsoon months compared to Lakhwar (a downstream station).

The impact of parameter uncertainty is assessed by analyzing the sensitivity of the parameters on the modeling outcomes using both manual and LH-OAT methods that perform LH sampling followed by OAT sampling (van Griensven et al., 2006). The analysis for the Upper Yamuna watershed identified snow formation and snow melt as well as soil-land use parameters as key determinants for evaluating the hydrological budget components based on limited available observed data. The watershed's area differentiation interpretation further confirms the relevance of the above parameters. The CN, AWC, TIMP, ESCO – which are functions of mean daily temperature, soil's permeability, land use, topography and antecedent soil water conditions – emerge as key sensitive parameters (Table 3). These parameters represent natural physical conditions prevalent in the watershed. CN influences the surface runoff. As infiltration decreases with increased surface runoff, baseflow and recharge are both inversely correlated to CN (Arnold et al., 2000). In the northern and eastern portions of the watershed comprising thick forests, the CN values were found to be lower than central and southern portions comprising arable land. The changes in AWC influence surface runoff, groundwater percolation, and water available for ET. As AWC increases, surface runoff decreases and/or percolation and water available for soil ET increases (Arnold et al., 2000). Also, with less storage, more water will either runoff or percolate and consequently, less water

Table 4
Results of sensitivity analysis of various parameters — groundwater recharge and nitrate leaching and groundwater quality modules.

Parameter	Description	Range used	Sensitivity
RCHRG_DP	Deep groundwater recharge fraction	0.04–0.2	High
SPYLD	Storage coefficient (Links fluctuation with recharge)	Lower aquifers: 0.0003–0.006 Shallow aquifers: 0.01–0.15	Moderate/high
Qaq (m day^{-1})	Groundwater discharge	0.001–0.005	Moderate/high
NPERCO	Nitrogen percolation coefficient	0.2–0.5	High
SOL_NO$_3$ (mg kg^{-1})	Initial nitrate concentration in soil layer	0.3–2.5	High
FRT_LY (kg ha^{-1})	Amount of Fertilizer applied	0.001–0.005	Moderate/high
GW_NO$_3$ (mgN l^{-1})	Initial nitrate concentration in ground water	0.3–1.5	Moderate
θ_e	Effective porosity	0.01–0.25	Moderate/high
K	Hydraulic conductivity (m day^{-1})	<1 to 50 m day^{-1}	Moderate/high
T	Transmissivity (m^2 day^{-1})	<10 to>3000 m^2 day^{-1}	
K$_v$	Denitrification coefficient (day^{-1})	0.00005–0.001	Moderate/high
α_l	Longitudinal dispersivity (m)	Universal scaling method (Neuman and Zhang, 1990)	Low
E$_l$	Coefficient of dispersion (m^2 day^{-1})	0.0000001–0.00001	Low

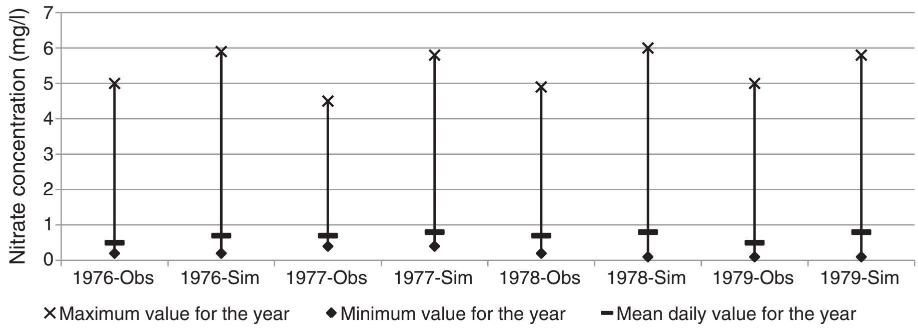

Fig. 6. Observed and simulated nitrate concentration (mg l^{-1}) at Lakhwar (Yamuna sub-basin) for calibration (1976–78) and validation (1979) periods.

will be available for ET. Incorporating multiple soil layers for the Upper Yamuna watershed further enabled depth distribution for evaporation influenced by ESCO. As values of ESCO decrease, it enables lower layers of soil matrix to compensate for the water deficit in the upper soil layers and causes higher soil ET. With an increase in the soil ET, there is less water available for surface runoff, baseflow, and recharge.

Water moves past the lowest depth of soil profile, flows through vadose zone before becoming aquifer recharge. Aquifer hydraulic conductivity (K), and storativity/specific yield (SPYLD) are primary calibration parameters for estimating groundwater flow (Table 4). Area-differentiated interpretation of the watershed enabled understanding of recharge (RCHRG_DP), K, and SPYLD. In the central and southern portions of the watershed comprising thicker layers of sand and gravel materials, the effective storativity value was found to be higher than the northern and western portions.

For analysis of the diffuse nutrient inputs (N), the distribution and fate of NO_3 in surface and groundwater systems could be determined by estimation of above components of the hydrological cycle. Use of an integrated modeling approach created a basis for this, since temporal and spatial distribution of NO_3 requires knowledge of precipitation distribution, runoff generation, groundwater recharge, and fertilizer application rate in addition to hydrochemistry of aquifers. The results obtained agree with Behrendt and Bachor (1998) in DeWit (2001) who demonstrated that nutrient load measured in the river network and the nutrient inputs in the basin are strongly related to total runoff in the basin. In the areas that are found to be dominated by direct runoff such as those in the north and part of central portions of the Upper Yamuna watershed, the intake of excess nitrogenous fertilizers from land to surface waters takes place after a short time after fertilizer application. Such areas are also less susceptible to nutrient leaching (Narula et al., 2002; Narula et al., 2003). Water conservation measures in such areas should focus more on contour bunding, small check dams and other surface water holding mechanisms. For these areas, it can also be expected that measures to reduce nutrient inputs into rivers will show impact on water quality after a short residence time. Regions located in the south, in which groundwater runoff is dominant, need to be considered differently. These areas have sandy loam-to-fine loamy soils and because of the low flow velocity of groundwater in aquifer systems, the input of nutrients into rivers will take place only after a longer residence time, even decades. Concentration of nitrates has been found to be high in these areas (Narula et al., 2003). Consequently, remediation measures here should focus more on balanced application of fertilizers.

For further investigations on the diffuse nutrient input into surface waters differentiated according to the runoff components, the different hydrochemical and hydrodynamic behavior of the nutrient has been considered in the study. Phosphate has the chemical tendency to be bound to soil particles. Thus, as a rule, it is not displaced by percolation water to groundwater systems. Therefore, the danger of phosphate percolation to groundwater is of minor importance. Instead, phosphate adsorbed on soil particles is washed off by direct runoff components. In areas where the direct runoff is high, there is an increased risk for phosphate intakes into surface waters. Heavy metals also depict a similar behavior of immobility and their transport is dominated by surface pathways.

The analysis of the NO_3 pollution risk needs to be carried out differently. Since NO_3 is not attracted to soil particles, its displacement is completely bound to flowing water. Parameters such as NPERCO that influence transport of nitrates and initial concentration on soil layer (SOL_NO_3) were sensitive parameters (Table 4). Consequently, areas where direct runoff predominates (mostly in north and central parts of the watershed) will have an actual short-term NO_3 hazard potential for surface waters, as long as the level of excess N is high and the N budget of the soils has not reached equilibrium after reduction of excess N fertilization. Where groundwater runoff predominates (mostly in south, central and western parts of watershed), a high pollution risk prevails for all areas depending on denitrification capacities in the aquifers.

Denitrification capacities in the aquifer can be determined by presence or absence of certain hydrochemical parameters, the most essential ones being Fe(II), Mn(II), oxygen (O_2), and org C in addition

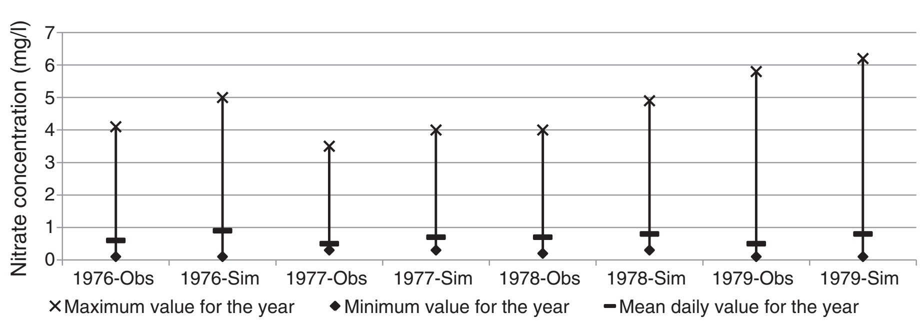

Fig. 7. Observed and simulated nitrate concentration (mg l^{-1}) at Yashwantnagar (Giri sub-basin) for calibration (1976–78) and validation (1979) periods.

to pH, hydrogen carbonate (HCO_3^-), K, and sulfate (SO_4^{2-}) content. Nitrate-degrading groundwater displays NO_3 contents of less than 1 mg l^{-1}, freedom from O_2, and high contents of Fe(II) and Mn(II) as a rule. In other words, groundwater aquifers that have low NO_3 content, low or nil O_2, high content of divalent ions, etc., invariably are expected to have high denitrification rates (Wendland, 1994). This combination of hydrochemical parameters has been used to determine the denitrification rate (K_v) as in Eq. (5),

$$K_v = K_{dn}\left(\frac{K_{O2,in\,hibitor}}{O_2 + K_{O_2,in\,hibitor}}\right)\left(\frac{Fe(II)}{K_{Fe} + Fe(II)}\right)\left(\frac{Mn(II)}{K_{Mn} + Mn(II)}\right)\left(\frac{org\,C}{K_C + org\,C}\right) \tag{5}$$

where, K_{dn} is the maximum denitrification rate in aquifers (day^{-1}), $K_{O2,inhibitor}$ is the half saturation rate for dissolved oxygen concentration (O_2) in groundwater aquifer (mg l^{-1}), K_{Fe}, K_{Mn} and K_c are half saturation rates of Fe(II), Mn(II), and organic carbon in groundwater aquifer respectively (mg l^{-1}). Fe(II), Mn(II) and org C are concentrations of divalent iron, manganese and organic carbon in aquifer (mg l^{-1}) (Narula, 2005; Conan et al., 2003).

Groundwater analysis in the Upper Yamuna watershed suggests that the aquifer is a non-nitrate degrading type mainly due to the absence of Fe(II) and Mn(II) that occur as a rule in reduced groundwater conditions in concentrations >0.2 mg l^{-1} as Fe(II), and >0.05 mg l^{-1} as Mn(II) respectively. In such areas denitrification coefficient (K_v) is very low implying that reduced inputs of nutrients as a result of a reduction of fertilizer use at the land surface will not immediately result in a reduced input to surface and groundwater (Table 4). This situation occurs mainly in areas such as southern and south-western portions of the Upper Yamuna watershed. In regions with a given denitrification capacity of groundwater (higher K_v) the pollution risk, as a rule, is of minor importance as long as groundwater residence times are large enough to enable complete denitrification of excess NO_3 fertilizer inputs. A certain risk, however, remains in the vicinity of rivers and other areas, mainly in central portions of the watershed.

The implications of projected climate change on components of hydrological cycle under different climate change scenarios, has been assessed for the Upper Yamuna watershed. Weather generated by A1B, A2 and B2 EC climate scenarios was transformed into hydrological regimes using the physically based integrated modeling techniques. The simulation results suggest that the future climate change will have a considerable impact on the runoff regimes. The seasonality of most of the investigated hydrological regimes will amplify. Based on the scenario analysis, the seasonal variability of most hydrological processes, such as runoff generation, ET as well as variables such as soil moisture, is likely to increase.

The implications of climate change are likely to increase average annual water yields under all scenarios for the Upper Yamuna watershed exhibiting increased variability in the seasonal availability of the water in the region. Higher temperatures in the Upper Yamuna watershed are likely to increase ET and therefore, the atmospheric vapor content. The increase in ET in the watershed is possible because of three reasons. First, the warmer climate increases the evaporation rate and secondly, the increase in precipitation enhances evaporation, and finally, the increase in the extent of snow-free area increases the evaporation because there is very little evaporation from the snow-covered area as compared with the snow-free area (Singh and Bengtsson, 2004). The changes in ET and the timing and intensity of precipitation are expected to affect various components of the hydrological cycle, particularly, soil moisture and groundwater storage. These trends would have implications on both economic and ecological aspects for agriculture: shift towards improved crop varieties, efficient irrigation, fertilizer management, and application of additional nitrogen.

Groundwater resources are related to climate change through the direct interaction with the surface water resources and recharge. The direct effect of climate change on groundwater resources depends on the change in the volume and distribution of groundwater recharge (a sensitive parameter as shown in Table 4). The lowering of groundwater tables is likely to be seen for the watershed with the declining contributions of groundwater to total water yield. Higher intensity rainfalls would lead to increase in surface runoff and reduction in the time for percolation and recharge. Such a situation will have implications for the irrigation requirements in the watershed, which are dependent on groundwater resources. Further, assuming the baseline conditions for contaminant loadings to remain the same, the likelihood of NO_3 concentrations in the groundwater of the Upper Yamuna watershed seems to be high. The implications of the above not only translate to health effects but also higher costs that are required for instituting measures for reduction of NO_3 pollution in groundwater (Almasri and Kaluarachchi, 2007).

Meanwhile, as also mentioned by IPCC, uncertainties in projections of future changes remain high, even if characterization of uncertainty has improved recently (IPCC, 2007b). Precipitation, the principal input signal to freshwater systems, is not adequately simulated in present climate models. Consequently, quantitative projections of seasonal changes in river flow at the basin scale, relevant to water management, remain largely uncertain (Milly et al., 2005; Nohara et al., 2006; Kundzewicz et al., 2008). The results of the present study are limited, by the above fact that three climate scenarios based on simulations of PRECIS–RCM and HadRM3–RCM have been used to derive the hydrological implications of climate change in the Upper Yamuna watershed. Consequently, even though climate change projections used in the study are limited by the above RCMs, they are moderated by the use of contrasting scenarios.

To ensure the projected changes, additional (validated) climate and hydrological models need to be applied in order to check the model sensitivity to climate change. Nevertheless the major trends projected by the integrated model used in the study are in the same direction for all scenarios. Therefore, the direction of changes does not seem to be questionable, only the intensity of change needs to be determined with increased certainty. Another aspect that needs to be recognized here is the limitation of the RCMs to properly represent elevation gradients.

As a consequence, locally important processes such as orographic precipitation and localized convective events that have implications for hydrology of the area tend to get neglected.

Recent studies have suggested the need for new frameworks for handling uncertainty to support decision-making processes. Pathways for identification of research needs would be, to focus on providing a better basis for decisions that must invariably be made under high uncertainty (Kundzewicz et al., 2008). These would include, for example, improved characterization of uncertainty (joint analysis of ensembles of climate models) that could assist water managers in their efforts to adapt to uncertain future hydrological changes.

5. Conclusions

This study presents the development and implementation of an integrated modeling framework capable of simulating flow of surface water, groundwater, and fate and transport of nutrients on a time-continuous basis for the Upper Yamuna watershed in northern India. The hydrological model SWAT, the groundwater model MODFLOW, and contaminant transport model MT3DMS were utilized for constructing the comprehensive integrated model. The study has been successful in calibrating and validating the integrated model. The simulated components of the hydrological cycle and NO_3 yields presented good Nash–Sutcliffe coefficients (>0.7).

The integrated model had the advantage of being fully distributed. An area-differentiated interpretation ensured that the integrated model corresponds well with the natural situations occurring in the watershed. Direct runoff (discharge) and groundwater recharge areas were suitably identified by combining the outcomes from the integrated model with area differentiated analysis. This combination further enhanced the understanding of fate and transport of nutrients into surface and groundwater according to the runoff components.

The combination of these three models not only led to accurate results but also consistent representation of the nitrogen-cycling processes. The kinetics of NO_3 transformation processes namely, nitrification and denitrification, both in the unsaturated soil zone and groundwater could be successfully represented. Denitrification capacities in the aquifer were determined through presence or absence of certain hydrochemical parameters.

Sensitivity analysis identified snow formation and snow melt as well as soil-land use parameters as key determinants for evaluating the hydrological budget components. Attention was paid to track limitations and uncertainties so that model results could be better appreciated.

Understanding the implications of climate change on various hydrologic, nutrient availability and transport components is of utmost importance for long-term and sustainable water resource planning. The kinetics of nutrient transformation processes for nitrogen that includes mineralization, nitrification and hydrolysis, volatilization, and denitrification is strongly influenced by environmental parameters such as soil moisture and temperature (Wendland, 1994; DeWit, 2001; Conan et al., 2003; Narula et al., 2003). For instance, as the soil moisture content increases and goes above the field capacity for an extended period, denitrification rates increase. Similarly, as soil temperature increases, the rate of denitrification increases.

Climate change scenarios show that the soil moisture stress is likely to increase in the future implying that rate of denitrification processes would decrease. This would further imply a reduction in natural removal of excess nitrogen from agricultural lands thereby leading to higher nitrate concentrations and loads getting transported to groundwater water systems in absence of appropriate water and nutrient management strategies. Future water and nutrient management strategies will have to focus on optimizing fertilizer application implying increase in efficiency of nitrogen and irrigation water use. A balanced fertilizer input will be required (WWF, 2010). Reduction in excessive use and application of chemical fertilizers such as urea, as well as improvement in supply-chain systems that ensure availability of organic fertilizers would also be required.

Climate change scenarios also project an increase in surface runoffs during the monsoon months with an increase in rainfall intensities. This would lead to increase in nutrient loss due to wash-off especially for phosphates and heavy metals that have chemical tendency to be bound to soil particles and get transported by surface pathways. This would again imply nutrient loss and reduction in nutrient availability for beneficial use. In brief, nutrient availability for beneficial agricultural use is likely to reduce while nutrient concentrations and loads transported to surface and groundwater systems are likely to increase unless proper management practices based on local environmental and hydrological conditions are considered.

The combination of a mountainous ecosystem and the amplified climate change illustrates the impact on streamflows, groundwater recharge and nutrient load distributions applicable to mountain areas. The water resource balance including quality that connects livelihoods of millions of people seems to be under increasing pressure due to the dynamic conditions of the natural environment and the future climate changes. The future research should focus on reducing uncertainty of climate projections and thereby their implications on hydrological and nutrient cycles, in order to formulate strategies/measures to altered seasonal hydrological conditions.

The study shows that the integrated SWAT–MODFLOW–MT3DMS model constitutes a valuable management tool that can be used to assess the impact of various anthropogenic and climate-related pressures.

Acknowledgments

We thank Prof. Subhash Chander, Former Deputy Director, Indian Institute of Technology (IIT) Delhi, and Professor, Department of Civil Engineering, IIT Delhi, for his constant help and constructive suggestions. We are also thankful to Ms. Shilpa Nischal for her efforts in helping us with data analysis and compilation of results. We sincerely thank the anonymous reviewers for providing valuable suggestions that have helped improve the paper.

References

Abbaspour KC, Yang J, Maximov I, Siber R, Bogner K, Mieleitner J. Modelling hydrology and water quality in the pre-alpine/alpine Thur watershed using SWAT. J Hydrol 2007;333:413–30.

Aggarwal PK. Global climate change and Indian agriculture: impacts, adaptation and mitigation. Indian J Agric Sci 2008;78(10):911–7.

Ahl RS, Woods SW, Zuuring HR. Hydrological calibration and validation of SWAT in a snow-dominated rocky mountain watershed, Montana, U.S.A. J Am Water Resour Assoc 2008;44(6):1411–30.

Almasri MN, Kaluarachchi JJ. Modeling nitrate contamination of groundwater in agricultural watersheds. J Hydrol 2007;343:21-229.

Amarasinghe UA, Shah T, Anand BK. India's water supply and demand from 2025–2050: Business-as-usual scenario and issues. In: Amarasinghe UA, Sharma BR, editors. Strategic analyses of the National River Linking Project (NRLP) of India, series 2. Proceedings of the Workshop on Analyses of Hydrological, Social and Ecological Issues of the NRLP. Colombo: International Water Management Institute; 2008. p. 23–60.

Arnold JG, Allen PM. Automated methods for estimating baseflow and groundwater recharge from streamflow records. J Am Water Resour Assoc 1999;35(2):411–24.

Arnold JG, Williams JR, Srinivasan R, King KW, Griggs RH. SWAT — Soil and Water Assessment Tool (User manual). Temple, TX: U.S. Department of Agriculture, Agricultural Research Service, Grassland Soil and Water Research Laboratory; 1996.

Arnold JG, Srinivasan R, Muttiah RS, Williams JR. Large area hydrologic modelling and assessment: I model development. J Am Water Resour Assoc 1998;34(1):73–89.

Arnold JG, Muttiah RS, Srinivasan R, Allen PM. Regional estimation of base flow and groundwater recharge in the Upper Mississippi River basin. J Hydrol 2000;227(1):21–40.

Bartarya SK. Hydrogeology and water resources of Intermontane Doon Valley. J Himalayan Geology 1995;6(2):17–28.

Behrendt H, Bachor A. Point and diffuse load of nutrients to the Baltic Sea by river basins of North East Germany (Mecklenburg-Vorpommern). Water Sci Technol 1998;38(10):147–55.

Buytaert W, Vuille M, Dewulf A, Urrutia R, Karmalkar A, Celleri R. Uncertainties in climate change projections and regional downscaling in the Tropical Andes: implications for water resources management. Hydrol Earth Syst Sci 2010;14:1247–58.

Chander S, Kapoor PN, Natarajan P, Gosain AK, Devi Rema, Shankar H. Newer techniques in high flow range forecasting. IIT Delhi, India: Department of Civil Engineering; 1984. p. 363.

Chapelle FH. Groundwater microbiology and geochemistry. New York: John Wiley and Sons; 1993. p. 424.

Chitale MA. Population and water resources of India. In: Gowarikar V, editor. Inevitable billion plus: science, population and development. Pune: Umesh Communications; 1992. p. 111–27.

Conan C, Bouraoui F, Turpin N, de Marsily G, Bidoglio G. Modelling flow and nitrate fate at catchment scale in Brittany (France). J Environ Qual 2003;32:2026–32.

CPCB (Central Pollution Control Board). Water Quality Status and Statistics (1974–2000), MINARS series.

DeWit MJM. Nutrient fluxes at the river basin scale I: the PolFlow model. Hydrol Processes 2001;15:743–59.

Engelman R, LeRoy P. Sustaining water: population and the future of renewable water supplies, population and environment program, population action international, Washington DC; 1993. p. 56. [Document Number PIP/092932].

Fertilizer Association of India (FAI), New Delhi (1970–2004). Fertilizer statistics (various issues).

Fontaine TA, Cruickshank TS, Arnold JG, Hotchkiss RH. Development of a snowfall-snowmelt routine for mountainous terrain for the soil water assessment tool (SWAT). J Hydrol 2002;262:209–23.

Galbiati L, Bouraoui F, Elorza FJ, Bidoglio G. Modeling diffuse pollution loading into a Mediterranean lagoon: development and application of an integrated surface-subsurface model tool. Ecol Model 2006;193(1–2):4-18.

Garg KK, Karlberg L, Barron J, Wani SP, Rockstrom J. Assessing impacts of agricultural water interventions in the Kothapally watershed, Southern India. J Hydrol Processes 2011. http://dx.doi.org/10.1002/hyp.8138. [Published online in Wiley Online Library (wileyonlinelibrary.com)].

Gassman PW, Reyes MR, Green CH, Arnold JG. The soil and water assessment tool: historical development, applications and future research directions. Trans ASAE 2007;50(4):1211–50.

Gosain AK, Rao S, Srinivasan R, Gopal Reddy N. Return-flow assessment for irrigation command in the Palleru river basin using SWAT model. Hydrol Processes 2005;19:673–82.

Gosain AK, Rao S, Srinivasan R, Basuray D. Climate change impact assessment on hydrology of Indian river basins. Curr Sci 2006;90(3):346–53.

Gosain AK, Rao S, Arora A. Climate change impact assessment of water resources in India. Curr Sci 2011;101(3):356–71.

Government of India. Draft National Water Policy 2012. Ministry of Water Resources; 2012. p. 33.

Harbaugh AW, McDonald MG. User's for MODFLOW-96, an update to the U.S. Geological Survey modular finite-difference ground-water model. U.S. Geol. Surv. Open-File Rep; 1996. p. 96-485.

Holvoet K, van Griensven A, Seuntjens P, Vanrolleghem PA. Sensitivity analysis for hydrology and pesticide supply towards the river in SWAT. Phys Chem Earth 2005;30:518–26.

IMD (India Meterological Department). Climatological table of observatories in India: 1951–1980; 1999.

Immerzeel WW, van Beck LPH, Bierkens MFP. Climate change will affect the Asian water towers. Science 2010;328:1382–5.

INAE (Indian National Academy of Engineering). Water resources management. Research Report; 2012. p. 170.

IPCC (Intergovernmental Panel on Climate Change). Special report on emission scenarios: summary for policy makers. Intergovernmental Panel on Climate Change; 2000 [21 pp.].

IPCC (Intergovernmental Panel on Climate Change) Summary for Policymakers. Climate change. In: Solomon S, Qin D, Manning M, Chen Z, Marquis M, Averyt KB, Tignor M, Miller HL, editors. The physical science basis. Contribution of working group I to the fourth assessment report of the intergovernmental panel on climate change; 2007b. p. 1-18.

IPCC (Intergovernmental Panel on Climate Change). Summary for Policymakers. Climate change. In: Parry ML, Canziani OF, Palutikof JP, van der Linden PJ, Hanson CE, et al, editors. Impacts, adaptation and vulnerability. Contribution of working Group II to the fourth assessment report of the intergovernmental panel on climate change; 2007a. p. 7-22.

Kelkar U, Narula KK, Sharma VP, Chandna U. Vulnerability and adaptation to climate variability and water stress in Uttarakhand State India. Global Environ Change 2008;18:564–74.

Krishna Kumar K, Patwardhan SK, Kulkarni A, Kamala K, Koteswara Rao K, Jones R. Simulated projections for summer monsoon climate over India by high-resolutio regional climate model (PRECIS). Curr Sci 2011;101(3):312–26.

Krysanova V, Becker A. Integrated modelling of hydrological processes and nutrient dynamics at the river basin scale. Hydrobiologia 2000;410:131–8.

Kumar R, Ghosh SK. Sedimentological studies of the upper Siwalik boulder conglomerate of Mohand area, Uttar Pradesh. J Himalayan Geology 1991;2(2):169–76.

Kundzewicz ZW, Mata LJ, Arnell NW, Doll P, Jimenez B, Miller K. The implications of projected climate change for freshwater resources and their management. Hydrol Sci J 2008;53(1):3-10.

Kunkel R, Wendland F, WEKU X. – a GIS supported stochastic model of groundwater residence times in upper aquifers for the supraregional groundwater management. Environ Geol 1997;30(1/2):1–9.

Li Z, Liu W, Zhang X, Zheng F. Impacts of land use change and climate change variability on hydrology in an agricultural catchments on the Loess Plateau of China. J Hydrol 2009;377:35–42.

McDonald MG, Harbaugh AW. A modular three-dimensional finite difference groundwater flow model. U.S. Geological Survey Techniques of Water-Resources Investigation Book 6, Chapter A1; 1988 [586 pp.].

Menking KM, Syed KH, Anderson RY, Shafike NG, Arnold JG. Model estimates of runoff in the closed, semiarid Estancia basin, central New Mexico, USA. Hydrol Sci J 2003;48(6):953–70.

Milly PCD, Dunne KA, Vecchia AV. Global pattern of trends in streamflow and water availability in a changing climate. Nature 2005;438:347–50.

Moors EJ, Groot A, Biemans H, van Scheltinga CT, Siderius C, Stoffel M, et al. Adaptation to changing water resources in the Ganges basin, northern India. Environ Sci Policy 2011;14:758–69.

Narula KK. GIS based area-differentiated supra-regional integrated hydrological and environmental modelling: application to Upper Yamuna river basin 2005; PhD thesis, Indian Institute of Technology, Delhi.

Narula KK, Lall U. Challenges in securing India's water future. J Crop Improvement 2010;24:85–91.

Narula KK, Bansal NK, Gosain AK, Wendland F. GIS based identification of risk to nutrient exposure in the large agriculture lands of India—towards better decision-making. Int J Environ Pollut 2002;2(6):82–94.

Narula KK, Bansal NK, Gosain AK, Wendland F. Area-differentiated modelling of excess nutrient and contaminant leaching risks at the river-basin scale using a hydrological approach in India. Int J Environ Pollut 2003;19(3):225–42.

Nash JE, Sutcliffe JV. River flow forecasting through conceptual models: part I A discussion of principles. J Hydrol 1970;10(3):282–90.

NATMO (National Atlas and Thematic Mapping Organization). District Planning Map Series. Summary of India District Planning Maps for districts of Simla, Sirmour, Solan, Uttarakashi, Tehri Garhwal, Dehradun and Yamunanagar. NATMO and Survey of India District Planning Series Maps. Government of India; 1996.

NBSS&LUP (National Bureau of Soil Survey, Land Use Planning). Soil series of India. NBSS Publication, 40. ; 1994. [683 pp.].

NCIWRDP (National Commission on Integrated Water Resources Development Plan). Integrated water resource development: a plan for action. Report of the NCIWRD, vol. I. New Delhi: Government of India, Ministry of Water Resources; 1999.

Neitsch SL, Arnold JG, Kiniry JR, Williams JR. Soil and water assessment tool theoretical documentation (Version 2000). Grassland, soil and water research laboratory, agricultural research service. Texas: Blackland Research Centre, Texas Agriculture Experimental Station; 2001.

Neitsch SL, Arnold JG, Kiniry JR, Williams JR, King KW. Soil and water assessment tool theoretical documentation (Version 2000). Temple, Texas: Grassland, Soil and Water Research Laboratory, Agriculture Research Service, Blackland Research Center, Texas Agricultural Experiment Station; 2002.

Neitsch SL, Arnold JG, Kiniry JR, Srinivasan R, Williams JR. Soil and water assessment tool input/output file documentation (version 2005). Temple, Texas: Grassland, Soil and Water Research Laboratory, Agriculture Research Service, Blackland Research Center, Texas Agricultural Experiment Station; 2005.

Neuman SP, Zhang YK. A quasi-linear theory of non-fickian and fickian subsurface dispersion, 2. Application to anisotropic media and the Borden site. Water Resour Res 1990;26(5):903–13.

Nohara D, Kitoh A, Hosaka M, Oki T. Impact of climate change on river runoff. J Hydromet 2006;7:1076–89.

Pauwels H, Kloppmann W, Foucher JC, Martelat A, Fritsche V. Field tracer test for denitrification in a pyrite-bearing schist aquifer. Appl Geochem 1998;13:767–78.

Rajeevan M, Bhate J, Kale JD, Lal B. High Resolution daily gridded rainfall data for the Indian region: analysis of break an active monsoon spells. Curr Sci 2006;91(3):296–306.

Shi PCC, Srinivasan R, Zhang X, Cai T, Fang X, Qu S. Evaluating the SWAT model for hydrological modeling in the Xixian watershed and a comparison with the XAJ model. Water Resour Manage 2011;25:2595–612.

Singh P, Bengtsson L. Hydrological sensitivity of a large Himalayan basin to climate change. J Hydrol Processes 2004;18:2363–85.

Singh P, Bengtsson L. Impact of warmer climate on melt and evaporation for the rainfed, snowfed and glacierfed basins in the Himalayan region. J Hydrol 2005;300:140–54.

Smedema LK, Rycroft DW. Land drainage—planning and design of agricultural drainage systems. New York: Cornell University press, Ithaca; 1983.

Sophocleous MA, Koelliker JK, Govindaraju RS, Berdie T, Ramireddygari SR, Perkins SP. Integrated numerical modelling for basin-wide water management: the case of the Rattlesnake Creek basin in south-central Kansas. J Hydrol 1999;214:179–96.

Srinivasan R, Ramanarayanan TS, Arnold JG, Bednarz ST. Large-area hydrological modelling and assessment: part II model application. JAWRA 1998;34(1):91-101.

Srinivasan R, Zhang X, Arnold J. SWAT ungauged: hydrological budget and crop yield predictions in the Upper Mississippi River basin. Trans ASAE 2010;53(5):1533–46.

State Ground Water Board. Groundwater development in the lower Yamuna region of Dehradun district, Uttaranchal. State Ground Water Board (SGWB) Report 42; 1982. p. 39.

van Griensven A. AVSWAT-X SWAT-2005 Advanced Workshop. SWAT 2005 3rd International Conference, Zurich, Switzerland; 2005.

van Griensven A, Meixner T, Grunwald S, Bishop T, Di Luzio M, Srinivasan R. A global sensitivity analysis tool for the parameters of multi-variable catchment models. J Hydrol 2006;324(1–4):10–23.

Wendland F. Die Nitratbelastung in den Grundwasserlandschaften der 'alten' Bundeslander (BRD). Berichte aus der Okologischen Forschung, Band 8. Juelich: Forschungszentrun Juelich; 1992. p. 150.

Wendland F. Modelling the nitrate flow in the ground-water provinces of the "old" federal states of the Federal Republic of Germany. Ecol Model 1994;75/76:385–97.

Williams JR, Jones CA, Dyke PT. A modelling approach to determining the relationship between erosion and soil productivity. Trans ASAE 1984;27(1):129–44.

World Wide Fund (WWF). Impacts of climate change on growth and yield of rice and wheat in the Upper Ganga Basin. http://awassets.wwfindia.org/downloads/impacts_of_climate_change_on_growth_and_yield_of_rice_and_wheat_in_the_upper_ganga_basin.pdf,2012-06-18 2010.

Zhang X, Srinivasan R, Debele B, Hao F. Runoff simulation of the headwaters of the Yellow River using the SWAT model with three snowmelt algorithms. J Am Water Resour Assoc 2008;44(1):48–61.

Zheng C, Bennett GD. Applied contaminant transport modelling: theory and practice. New York: Van Nostrand Reinhold; 1995 [440 pp.].

Zheng C, Wang PP. MT3DMS: a modular three-dimensional multispecies transport model for simulation of advection, dispersion, and chemical reactions of contaminants in groundwater systems; documentation and user's guide SERDP-99-1. Washington, DC: U.S. Army Corps of Engineers; 1999.